A Compact Multi-faceted Reflectarray based-on Cassegrain Optics

Borja Imaz-Lueje[1], David González-Ovejero[2], Marcos R. Pino[1], Manuel Arrebola[1], Ronan Sauleau[2]
[1] Group of Signal Theory and Communications, University of Oviedo, Spain, {bimaz, mpino, arrebola}@uniovi.es
[2] Univ. Rennes, CNRS, IETR, (Institut d'Electronique et des Technologies du numérique) - UMR 6164, Rennes, F-35000, France, {david.gonzalez-ovejero, ronan.sauleau}@univ-rennes1.fr

***Abstract*—This paper presents a compact Cassegrain reflector antenna in which a multi-faceted reflectarray plays the role of main reflector. The reflectarray surface is composed by three identical panels, arranged following a cylindrical-parabolic structure. The designed antenna provides a dual linear polarization (LP) and radiates a pencil around a center frequency of 31 GHz. The performance of this antenna is evaluated and compared with an equivalent single-facet Cassegrain reflectarray. The sectorization in the multi-faceted structure relaxes the phase requirements to be provided by the unit-cell, which reduces the phase errors in simple cell topologies. The multi-faceted structure achieves a better performance in terms of gain bandwidth, showing an improvement of at least 30% in the relative bandwidth and 50% in the gain-bandwidth product regarding a conventional single-facet reflectarray.**

***Index Terms*— Compact reflector antennas; Cassegrain system; reflectarrays; multi-faceted structures;**

I. Introduction

Cassegrain reflectors [1] have been pervasively used in space applications such as satellite communications, remote sensing, and radio astronomy. Traditionally, they consist of a feed, a main parabolic reflector, and a hyperboloid sub-reflector, which is designed to optimize the illumination of the paraboloid. The advantages of these structures lie in the reduction of the antenna volume and height in comparison with front-fed or single-offset reflector arrangements, as well as an improvement of the antenna efficiency and side radiation [2].

The use of printed reflectarrays [3] as main reflector constitutes an interesting solution to further reduce the volume and weight of Cassegrain reflectors. Owing to their similar optics behavior, planar shape, and low-profile, these surfaces can substitute the parabolic reflector in a Cassegrain antenna, providing a lightweight approach. The use of reflectarrays in Cassegrain configurations has been proposed in several applications such as mm-wave terrestrial communications [4]-[6] or satellite communications [7],[8].

Despite their attractive features, printed reflectarrays are impaired by a somehow narrow bandwidth of gain [9]. Such limitation is mainly due to two reasons: the bandwidth of the radiating element and the spatial phase delay effect. Several works have proposed different strategies to mitigate these issues. At the unit-cell level, multi-resonant or complex cell topologies [10] - [12] achieve better in-band performance. The use of true-time delay unit-cells [13] or optimizations on the geometry of the cell [14],[15] can also improve the overall antenna bandwidth. Alternatively, the use of structures with higher f/D ratios can reduce the spatial phase delay effect [3], at the expense of increasing the overall antenna volume. Finally, multi-faceted [16],[17] or parabolic reflectarrays [18] efficiently exploits their resemblance with a parabolic profile to improve the bandwidth of the antenna.

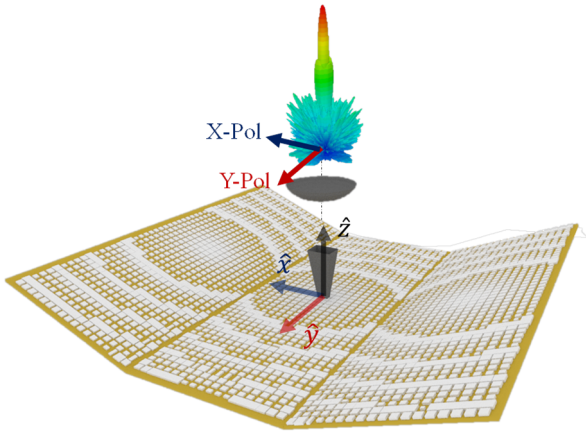

Fig. 1. 3D view of the proposed dual reflector reflectarray.

This contribution presents a Cassegrain reflectarray where the main reflector consists of a multi-faceted reflectarray. The facets of the reflector follow a parabolic cylinder to mitigate the differential spatial phase delay. The antenna radiates in dual-linear polarization (X and Y polarizations) a broadside pencil beam at Ka-band. The design and analysis of the Cassegrain reflectarray has been carried out using a Method of Moments based on Local Periodicity (MoM-LP) [19]. Besides, the effect of the sub-reflector is considered during the calculation of the reflector illumination. A comparison between the multi-faceted structure and single-facet Cassegrain reflectarray of an equivalent aperture is also reported.

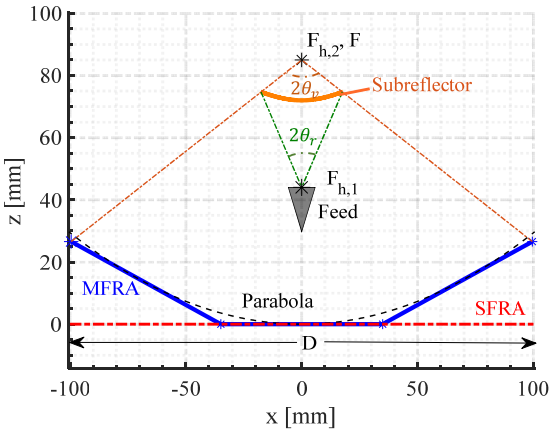

Fig. 2. Optics of the proposed Cassegrain reflectarrays in the XZ plane: Multi-faceted (MFRA), blue solid line and single-facet (SFRA) red dashed line.

II. Multi-Faceted Cassegrain Reflectarray Design

A. Antenna Optics & Cassegrain Configuration.

Fig. 1 shows a perspective view of the proposed Cassegrain multi-faceted reflectarray, whereas Fig. 2 depicts a side view for both the Multi-Faceted (MFRA) and the Single-Facet (SFRA) one. The antenna consists of three parts: a dual-polarized feed, a sub-reflector, and the main reflector. The latter is a multi-faceted reflectarray composed of three identical panels; the lateral panels present mirror symmetry along the YZ plane and are inclined an angle of 22.4º considering the central one, according to a parabolic profile (dashed black line in Fig. 2) in the XZ plane. The focus of this parabola is $F = 85$ mm. Each panel is made of 936 unit-cells distributed in a rectangular lattice of 18 x 52 elements. Thus, the equivalent aperture of the reflectarray is 199.0 x 201.8 mm^2. Following the same antenna optics, the equivalent single-facet reflectarray consists of 2704 elements, distributed also in a rectangular lattice of 52 x 52 elements.

The feed aperture is located above 44 mm the main reflector surface. This source is modeled using an ideal $\cos^q \theta$ function. At the design frequency (31 GHz), q is equal to 7.9 both the E- and the H-planes and varies linearly in-band. The feed is a single linearly-polarized source, so to generate the double polarization it is rotated regarding the z-axis of Fig. 1. In this manner, the E-plane of the feed is aligned with the x-axis and y-axis to generate the X and Y polarizations respectively (see Fig. 1). The sub-reflector consists of a metallic hyperbola with diameter 35.11 mm, which corresponds to a $0.17D$ (being D the size of the aperture in the XZ plane, as shown in Fig. 2) so the blockage produced by the sub is expected to be small [2]. The vertex of the hyperbola is 72 mm above the main reflector and the focal points are located at $F_{h,1} = 44$ mm and $F_{h,2} = 85$ mm as shown in Fig. 2. In this configuration, the subtended angle between the sub and the main reflector (θ_v) is 59.6º and the angle between the feed and the hyperbola (θ_r) is 29.8º.

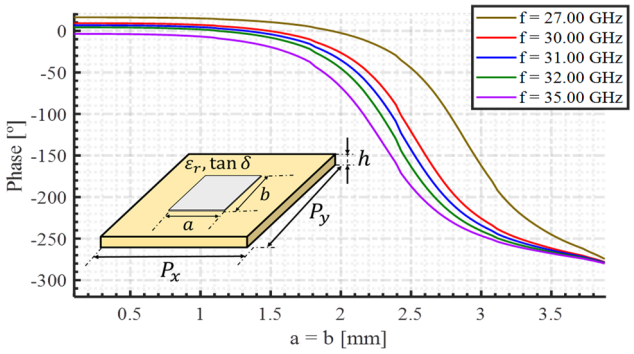

Fig. 3. Unit-cell geometry and phase response of the unit-cell as a function of the patch size for different frequencies under normal incidence.

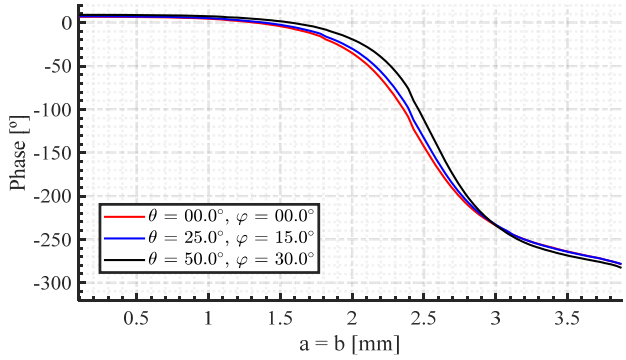

Fig. 4. Phase response of the unit-cell as a function of the patch size for different angles of incidence at 31.00 GHz.

Both reflectarrays have an f/D ratio of 0.43 and a compactness (calculated as the ratio of the height of the sub-reflector and the reflectarray aperture) of 0.36.

B. Unit cell characterization.

The radiating element (see Fig. 3) is a single-layer variable-size rectangular patch backed by a ground plane. The patch is printed on substrate duroid5880 ($\varepsilon_r = 2.30; \tan\delta = 0.003$) whose thickness is $h = 0.762$ mm. The inter-element spacing is 3.88 mm in both axis, which corresponds to $0.4\lambda_0$ at the design frequency. This cell topology provides the phase response shown in Fig. 3 and Fig. 4. Between 1.3 and 3.8 mm, the phase curve introduced by the unit-cell has a maximum range of 280º. This curve is robust under different angles of incidence and in-band, at frequencies close to the designed one. At frequencies further away (27 and 35 GHz), the deviation of the curve regarding the behavior at 31 GHz starts to be significant.

C. Layout Design &Analysis Procedure.

To collimate a beam in a given direction of space (θ_0, φ_0), the phase-shift introduced by each unit-cell is given by,

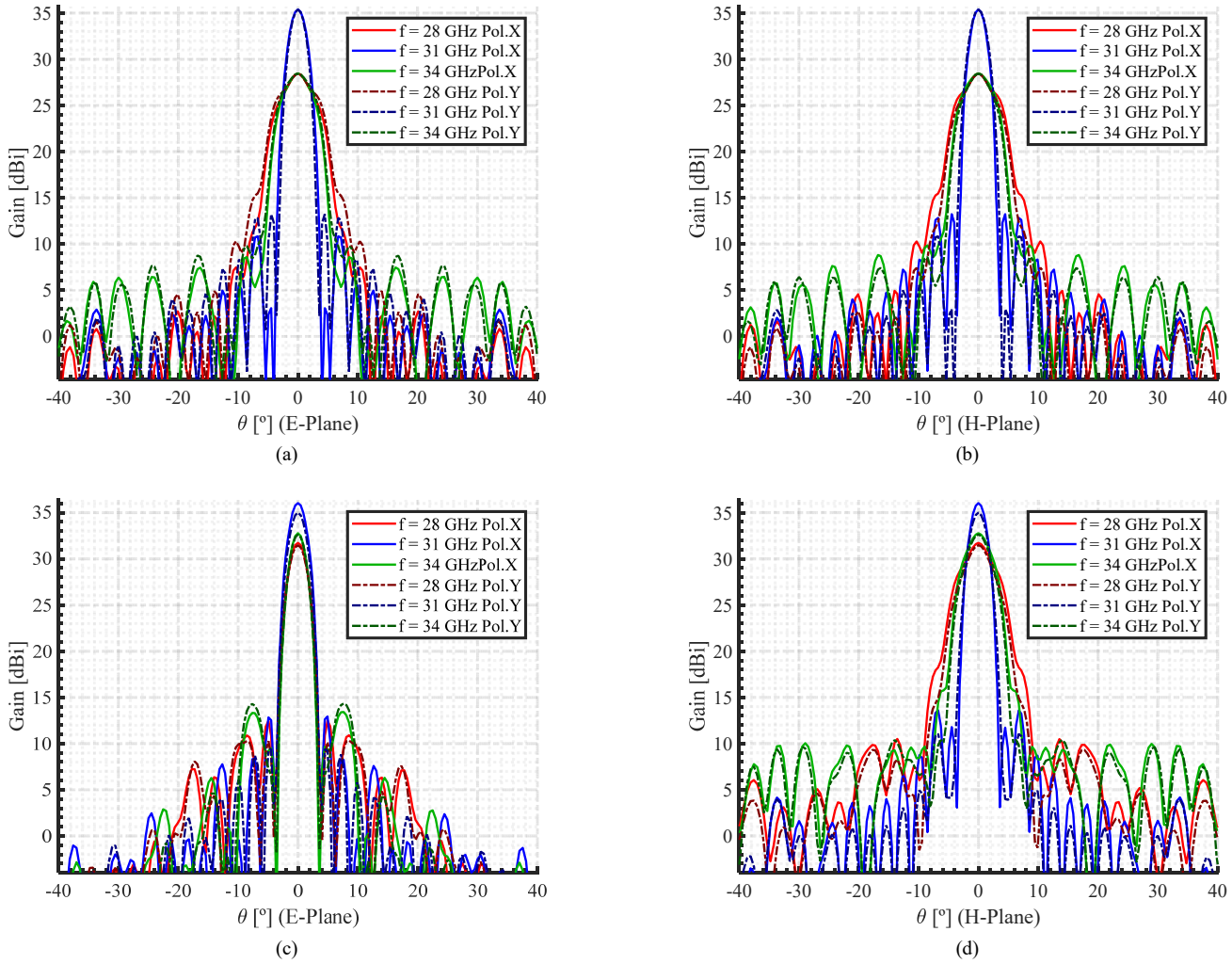

Fig. 5. Gain patterns of the reflectarray designs at the design frequency (31.0 GHz) over a 6 GHz bandwidth. E-plane (a) and H-plane (b) cuts of single-facet reflectarray. E-plane (c) and H-plane (d) of the multi-faceted reflectarray. Dotted lines correspond to the field in Y polarization and solid ones to X polarization.

$$\phi(\vec{r}_i) = k_0[d_i - (x_i \sin\theta_0 \cos\varphi_0 + y_i \sin\theta_0 \sin\varphi_0 + z_i \cos\theta_0], \quad (1)$$

where $\vec{r}_i = (x_i, y_i, z_i)$ are the coordinates of the i-th reflectarray element, k_0 is the wavenumber in vacuum and d_i is the distance between the element and the focus of the equivalent parabola. Considering the coordinate system shown in Fig. 2, one may calculate the phase distribution required in each panel of the designs to generate a broadside beam ($\theta_0 = 0.0°$, $\varphi_0 = 0.0°$). The design process is carried out element by element, using the MoM-LP in [19] and considering the real incidence angle on each cell. Here, the dimensions a and b of the patch are adjusted to generate the phase required on each polarization. Fig. 1 shows the resulted layout for each panel of the MFRA. These layouts in the sectorization plane XZ present a smooth variation in the patch sizes. This reduces the number of phase wraps (or equivalently of abrupt variation in the size of contiguous patches) which has a negative impact in the radiation pattern of the antenna in-band [20]. The smoother variation in the dimensions of the unit-cell along the sectorization axis is a characteristic behavior in multi-faceted reflectarrays which is due to the phase distribution required in each panel [17]. In the non-sectorized cut, the multi-faceted reflectarray has more patch size variation in the same way as a conventional reflectarray.

III. Multi-Faceted Reflectarray Performance

To assess the performance of both Cassegrain reflectarrays (i.e. the MFRA and the SFRA), the dual-reflector configuration depicted in Fig. 2 is replaced by a single reflector model, where the feed and sub-reflector are replaced by an equivalent feed located at the focus of the parabola. Because of the convex curvature of the sub-reflector, the equivalent feed has a broader beamwidth than the original one. According to [21], the ratio between the beamwidths of the equivalent and original feed can be calculated with the ratio between the angles θ_v/θ_r. Using this equivalent model, the

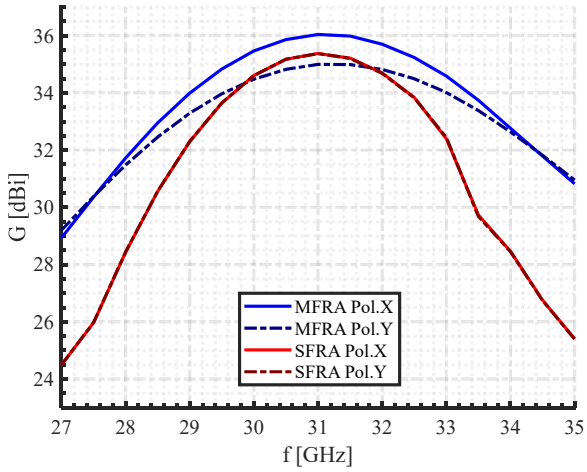

Fig. 6. Gain from 27 to 35 GHz for multi-faceted (MFRA) and single-facet (SFRA) Cassegrain configurations. Dotted lines correspond to the Y polarization and solid ones to the X polarization.

TABLE I. MULTI-FACETED VS. SINGLE-FACET GAIN BANDWIDTH

Design	SFRA		MFRA	
	Pol. X	Pol.Y	Pol. X	Pol.Y
G_{max}	35.4 dBi	35.4 dBi	36.0 dBi	35.0 dBi
BW_{1dB}	2.2 GHz (7.10%)	2.2 GHz (7.10%)	2.9 GHz (9.37 %)	3.6 GHz (11.61%)
GBP (1 dB)	24618	24618	37303	36714
BW_{3dB}	4.0 GHz (12.90%)	4.0 GHz (12.90%)	5.3 GHz (17.10%)	5.7 GHz (18.40%)
GBP (3 dB)	44729	44729	68076	58186

performance of both designs has been evaluated using the MoM-LP [19] and the methodology explained in [17].

Fig. 5 presents the gain patterns for each polarization of the Cassegrain reflectarrays. At the central frequency of 31 GHz, both designs achieve a broadside beam with at least 35 dBi gain. The side lobe levels are also similar in both reflectarrays, being at least 20 dB below the maximum. In-band, some differences appear between reflectarray designs. In the non-sectorized plane (YZ plane), both antennas show a significant degradation in the main beam shape due to the errors introduced by the phase wraps. Conversely, the multi-faceted configuration yields a more stable beam in the sectorization plane (XZ plane) compared to the single-facet version. The gain levels in both designs are reduced as one moves away from the central frequency, although the MFRA achieve higher gain levels in comparison to the SFRA.

Fig. 6 and Table I show the maximum gain of the reflectarrays evaluated at 31 GHz (G_{max}) and in a wider range of frequencies (27 – 35 GHz). The trend in gain mentioned above is also observed in this band. In both polarizations, the multi-faceted design achieves more stable gain levels compared to the equivalent single-facet one. The response of both polarizations in the SFRA is almost the same but, in the multi-faceted case, some differences between polarizations are shown. The X polarization achieves a higher level of gain at design frequency, while the Y polarization has a flatter in-band response.This behaviour is due to the illumination of each one of the reflectarray panels, which is different for each polarization.

To quantify the improvement in the antenna performance, Table I shows the calculated bandwidth for each design and polarization, according to the 1 dB and 3 dB gain drop. Regarding the bandwidth achieved in the single-facet, the multi-facet reflectarray achieves a bandwidth improvement of 32% in the X polarization and 64% in the Y polarization. In addition, Table I shows the Gain-Bandwidth Product (GBP). This is calculated as,

$$GBP(x\ dB) = BW_{xdB}(\%) \cdot 10^{G_{max}/10} \quad (2)$$

where x is the gain drop considered (1 or 3); $BW_{xdB}(\%)$ is the bandwidth of the antenna relative to the design frequency and G_{max} the peak gain at this frequency. In both polarizations and for both drop gain, the MFRA achieves a GBP 50% higher than that obtained in the SFRA.

IV. CONCLUSIONS

A compact multi-faceted reflectarray structure based-on a Cassegrain feeding has been designed and evaluated. The structure consists of three panels which follows a parabola on one axis to mitigate the spatial phase delay and therefore improve the bandwidth of a conventional reflectarray. The multi-faceted reflectarray is illuminated by a Cassegrain configuration of feed plus sub-reflector, resulting in a compact solution. The antenna has been designed to radiate a pencil beam in dual-linear polarization at 31 GHz. The performance of the multi-faceted antenna is compared with an equivalent single-facet reflectarray.

The multi-faceted structure yields a smooth variation in the size of the radiating elements along the axis where sectorization is applied. The effect is due to the reduction in the phase range required on each panel to collimate the beam. Since the unit cell used has a phase range lower than a full cycle (360º), the error between the ideal phase needed on the reflectarray surface and those provided by the unit-cell is reduced.

Regarding the shape of the radiation pattern, although a similar behavior has been observed in the non-sectorized axis, the multi-faceted antenna presents an in-band stability better than the single-facet version. Besides, the multi-faceted reflectarray maintains higher in-band gain levels than the single-facet case for both polarizations. This means an increase in antenna bandwidth, thus resulting in a significant improvement in the gain-bandwidth ratio.

This work demonstrates that multi-faceted reflectarrays, when they are used in a Cassegrain configuration, improve the gain bandwidth ratio regarding a conventional reflectarrays

without impacting the compactness of the structure. Therefore, the multi-faceted structure presented is amenable for deployment and constitute an interesting solution for small platforms in space applications.

ACKNOWLEDGMENT

This work was supported in part by MICIN/AEI/10.13039/501100011033 within the projects PID2020-114172RB-C21 and TED2021-130650B-C22; by Gobierno del Principado de Asturias under project AYUD/2021/51706; and by Spanish Ministry of Education under grant FPU18/0575.

REFERENCES

[1] P. W. Hannan , "Microwave antennas derived from the Cassegrain telescope" *IRE Trans. Antennas Propagat*., vol. AP-9, March 1961, pp. 140-153.

[2] K. S. Rao and P. S. Kildal, "A study of the diffraction and blockage effects on the efficiency of the Cassegrain antenna," in *Can. Electr. Eng. J.,* vol. 9, no. 1, pp. 10-15, Jan. 1984, doi: 10.1109/CEEJ.1984.6591356.

[3] J. Huang and J. A. Encinar, Reflectarray Antennas, John Wiley & Sons, Hoboken, NJ USA, 2008, ISB: 978-0-470-08491-5.

[4] R. S. Hao, Y. J. Cheng, Y. F. Wu and Y. Fan, "A W-Band low-profile dual-polarized reflectarray with integrated feed for in-band full-duplex application," *IEEE Trans. Antennas Propag.*, vol. 69, no. 11, pp. 7222-7230, Nov. 2021, doi: 10.1109/TAP.2021.3109641.

[5] M. R. Chaharmir, J. Shaker, M. Cuhaci and D. Lee, "Development of a dual band circularly-polarized cassegrain microstrip reflectarray," *Int. Symp. Antenna Technolo. Appl. Electromagn. URSI Conf.*, 2004, pp. 1-4, doi: 10.1109/ANTEM.2004.7860588.

[6] G. -B. Wu, S. -W. Qu and S. Yang, "Low-profile transmitarray antenna with Cassegrain reflectarray feed," in *IEEE Trans. Antennas Propag.,* vol. 67, no. 5, pp. 3079-3088, May 2019, doi: 10.1109/TAP.2019.2899029.

[7] C. Han, J. Huang and K. Chang, "Cassegrain offset subreflector-fed X/Ka dual-band reflectarray with thin membranes," in *IEEE Trans. Antennas Propag.* vol. 54, no. 10, pp. 2838-2844, Oct. 2006, doi: 10.1109/TAP.2006.882176.

[8] N. Chahat, G. Agnes, J. Sauder and T. Cwik, "One meter deployable reflectarray antenna for earth science radars," *IEEE Int. Symp. Antennas Propag. USNC/URSI Nat. Radio Sci. Meet.,* 2017, pp. 245-246, doi: 10.1109/APUSNCURSINRSM.2017.8072165.

[9] J. Huang, "Bandwidth study of microstrip reflectarray and a novel phased reflectarray concept", *IEEE Int. Symp. Antennas Propag..*, Newport Beach, California, pp. 582-585, June 1995.

[10] J. A. Encinar and J. A. Zornoza, "Broadband design of three-layer printed reflectarrays," in *IEEE Trans. Antennas Propag.*, vol. 51, no. 7, pp. 1662-1664, July 2003, DOI: 10.1109/TAP.2003.813611.

[11] L. Moustafa, R. Gillard, F. Peris, R. Loison, H. Legay and E. Girard, "The Phoenix Cell: a new reflectarray cell with large bandwidth and rebirth capabilities," in IEEE *Antennas Wireless Propag. Letter*, vol. 10, pp. 71-74, 2011, doi: 10.1109/LAWP.2011.2108633.

[12] M. R. Chaharmir, J. Shaker and H. Legay, "Broadband design of a single layer large reflectarray using multi cross loop elements," in *IEEE Trans. Antennas Propag.,* vol. 57, no. 10, pp. 3363-3366, Oct. 2009, doi: 10.1109/TAP.2009.2029600.

[13] E. Carrasco, J. A. Encinar and M. Barba, "Wideband reflectarray antenna using true-time delay lines," *2nd Eur. Conf. Antennas Propag.*, *EuCAP*, 2007, pp. 1- 6, DOI: 10.1049/ic.2007.0939.

[14] D. R. Prado, M. Arrebola, M. R. Pino and G. Goussetis, "Broadband reflectarray with high polarization purity for 4K and 8K UHDTV DVB-S2," in *IEEE Access*, vol. 8, pp. 100712-100720, 2020, doi: 10.1109/ACCESS.2020.2999112.

[15] M. Zhou, O. Borries and E. Jørgensen, "Design and optimization of a single-layer planar transmit-receive contoured beam reflectarray with enhanced performance," in *IEEE Trans. Antennas Propag.*, vol. 63, no. 4, pp. 1247-1254, April 2015, doi: 10.1109/TAP.2014.2365039..

[16] H. Legay, D. Bresciani, E. Labiole, R. Chiniard, R. Gillard, "A multi facets composite panel reflectarray antenna for a space contoured beam antenna in Ku band", *Prog. Electromagn. Res. B*, vol. 54, pp 1- 26, 2013.

[17] B. Imaz-Lueje, Marcos R. Pino, Manuel Arrebola, "Deployable multi-faceted reflectarray antenna in offset configuration with band enhancement" *IEEE Trans. Antennas Propag.*, 2022, doi: 10.1109/TAP.2022.320975.

[18] D. Martinez-de-Rioja et al., "Transmit–receive parabolic reflectarray to generate two beams per feed for multispot satellite antennas in Ka-Band," in *IEEE Trans. Antennas Propag.*, vol. 69, no. 5, pp. 2673-2685, May 2021, doi: 10.1109/TAP.2020.3030942.

[19] C. Wan, J. A. Encinar, "Efficient computation of generalized scattering matrix for analyzing multilayered periodic structures" *IEEE Trans. Antennas Propag*., vol. 43, pp. 1233 – 1242, 1995.

[20] R. E. Hodges, J. C. Chen, M. R. Radway, L. R. Amaro, B. Khayatian and J. Munger, "An extremely large Ka-band reflectarray antenna for Interferometric Synthetic Aperture Radar: enabling next-generation satellite remote sensing," *IEEE Antennas Propag. Mag.*, vol. 62, no. 6, pp. 23-33, Dec. 2020, doi: 10.1109/MAP.2020.2976319.

[21] Constantine A. Balanis, Antenna Theory: Analysis and Design, John Wiley & Sons, Hoboken, NJ USA, 2005, ISB: 978-0-470-08491-5.